18th NORTH SEA FLOW MEASUREMENT WORKSHOP 2000

THE DISCHARGE COEFFICIENT AND THROUGH-LIFE PERFORMANCE OF VENTURI TUBES

Dr M J Reader-Harris, Mr N Barton, Mr W C Brunton, Mr J J Gibson, Dr D Hodges, Mr I G Nicholson and Mr P Johnson
National Engineering Laboratory

1 INTRODUCTION

Until recently it was generally assumed that the discharge coefficient of a Venturi tube is constant provided that the pipe Reynolds number is greater than around 2×10^5. However, recent work has shown the problems with this view. The work of Jamieson et al [1] and of van Weers et al [2] has shown that the performance of Venturi tubes in gas is very different from that in water. This paper describes experimental work carried out on new Venturi tubes in water and dry gas and gives a partial explanation of the behaviour of the discharge coefficient in gas. This work was supported by the National Measurement System Policy Unit of the Department of Trade and Industry.

The second problem which this paper addresses is the extent to which the discharge coefficient can change with time. Operating in a harsh environment the internal geometry of the Venturi tube may deteriorate owing to corrosion or erosion. In particular the Venturi tube may roughen. This will affect the accuracy of the flow measurement. This part of the work reported here was done using computational fluid dynamics (CFD) and was funded by a Joint Industry Project (JIP) supported by Elf Exploration, Jordan Kent Metering Systems/Seiko, Mobil North Sea, and Shell International.

There is an increasing desire to use Venturi tubes for wet gas measurement, and major projects on Venturi tubes are being undertaken at NEL in order to determine their performance. However, it is necessary to understand their behaviour in dry gas first.

2 EXPERIMENTAL WORK

2.1 Description of the Venturi Tubes

Fifteen classical Venturi tubes with machined convergent sections were manufactured by Jordan Kent Metering Systems/Seiko and Crane Perflow for calibration in water and in gas: the former manufacturer manufactured Venturi tubes with diameter ratio β = 0.4, 0.6 and 0.75 for nominal diameter 50 mm, 100 mm and 200 mm, together with β = 0.5, 0.65 and 0.7 for nominal diameter 100 mm only; the latter manufactured Venturi tubes with β = 0.4, 0.6 and 0.75 for nominal diameter 100 mm only. They were manufactured to drawings with tight tolerances designed to ensure that where possible the results were not affected by uncontrolled variables. Each Venturi tube was manufactured out of solid metal so that there would be no steps due to welding within the Venturi tube. They were made of stainless steel and were suitable for use at pressures up to 70 bar with ANSI Class 600 flanges. They were designed not only to meet the requirements of ISO 5167-1 [3] but to follow its recommendations. The Standard recommends the use of a divergent angle between 7° and 8°: 7½° was specified for the Venturi tubes used in this project.

So that the results would not be corrupted by the introduction of steps at joins in the pipework, an upstream length of 8*D* (6*D* for 200 mm pipe) and a downstream length of 4*D*, where *D* is the diameter of the entrance cylinder, were manufactured with machined bores; this ensured that in no case was there a step in diameter greater than 0.0035*D* at the upstream flange of the Venturi tube. The lengths of pipework were manufactured by boring out Schedule 80 pipe to the bore of

a Schedule 40 pipe. The lengths of pipe and the Venturi tubes were dowelled to ensure concentricity; O rings were used to ensure that there would not be recesses or protruding gaskets. The distance from the upstream pressure tappings to the first upstream flange was 1.5*D*, 1.1*D* and 0.7*D* for nominal diameters of 50 mm, 100 mm and 200 mm respectively.

In addition to the shorter lengths of pipework already described, an additional 21*D* (23*D* of 200 mm pipe) length was manufactured by welding a 19*D* (21*D* of 200 mm pipe) length of Schedule 40 pipe to a 2*D* length of pipe machined to the bore of the other pipes, smoothing off any step at the weld. This length of pipe was installed with the machined length adjacent to the machined pipe already described, so that there was at least 8*D* of machined pipework, whose bore matched that of the Venturi tube very accurately, immediately upstream of the Venturi tube. In total there was 29*D* of pipe of the same schedule with no recesses, protruding gaskets or significant steps upstream of the Venturi tube. Upstream of this assembly there was generally further pipe of the same nominal diameter preceded by a flow conditioner.

The Standard recommends that the radii of curvature at the intersections of the entrance cylinder and the convergent section, the convergent section and the throat, and the throat and the divergent section be equal to zero, although significantly larger values are permitted. The drawings requested a maximum radius of curvature of 1 mm. In order to measure the radius of curvature measurements of profile were made through the convergent and the throat with one trace per Venturi tube. This was not possible for some of the Venturi tubes. The average of the measured radii of curvature was 17 mm.

The Standard requires that the surface finish of the entrance cylinder, the convergent section and the throat be such that R_a/d shall always be less than 10^{-5}, where R_a is the arithmetical mean deviation of the roughness profile. However, this was typically exceeded by a factor of approximately 3; the typical surface finish was $R_a \approx 1.7$ μm. All the Venturi tubes had $10^{-5} < R_a/d < 10^{-4}$. If the Draft International Standard proposed to replace ISO 5167-1 is accepted the maximum permissible roughness will be increased so that R_a/d shall be less than 10^{-4}. The project wished to use Venturi tubes with surface roughnesses typical of those used in the field. Moreover, the range of roughnesses does not appear to be the cause of the spread in measured discharge coefficients.

Except for the Venturi tube with a throat diameter of 20 mm the pressure tappings were 4 mm in diameter; the throat pressure tappings were of constant diameter for a length of 94 mm and the upstream tappings for a length of 53 mm. The Venturi tube with a throat diameter of 20 mm had pressure tappings of diameter 2.6 mm; the throat pressure tappings were of constant diameter for a length of 62 mm and the upstream tappings for a length of 37 mm. Tappings of constant diameter were used because the work described by Jamieson et al suggested that they might be beneficial. The tappings were connected in 'triple-tee' arrangements.

For most of the Venturi tubes the convergent angles were determined both from three measurements of diameter for each convergent cone and from the wall profile measurements from which intersection radii were obtained. The measured value of the convergent angle never differed from the nominal value by more than 0.14º.

Except for one measured diameter in the 20 mm throat (nominal diameter 50 mm, $b = 0.4$) the measured throat diameters were within 0.1 per cent of the mean value of the throat diameters at the pressure tappings. The measured diameters of the entrance cylinders were within 0.05 per cent of the mean value of the entrance cylinder diameters at the pressure tappings.

2.2 Calibration in Water

The Venturi tubes were calibrated in water in the UKAS-accredited National Standard facility for water flow measurement. For each Venturi tube the data in water lay on a straight line and with a small scatter. The slopes were small: when fitted against Re_D the majority had a positive sign but since several had a negative sign it seemed appropriate to represent the discharge coefficient of each Venturi tube by its mean value. Over the range of the data the average

increase in discharge coefficient with Reynolds number was 0.0005. The results for the standard Venturi tubes are shown in Figure 1. Where two Venturi tubes are made from the same drawings the maximum difference in mean discharge coefficient is 0.57 per cent. The Reynolds number range over which the data were used to calculate the mean was that over which C was approximately constant. In one case there was a significant hump in the data for $1.2 \times 10^5 < Re_D < 2 \times 10^5$; the throat Reynolds number below which C decreased rapidly varied but was typically about 2.5×10^5.

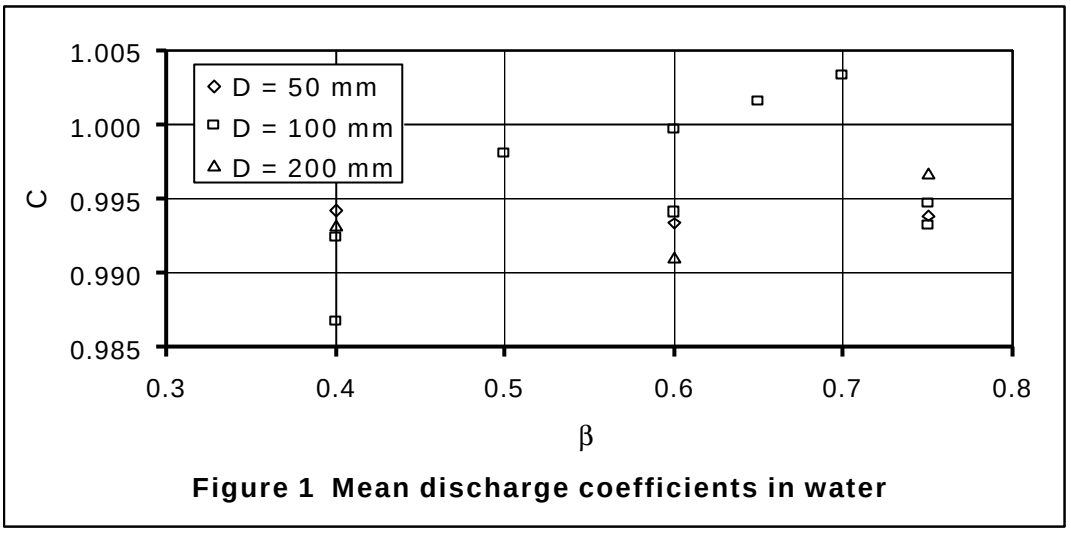

Figure 1 Mean discharge coefficients in water

Fitting the data in Figure 1 gives an equation for C in water of

$$C_{water} = 0.9878 + 0.0123b. \quad (1)$$

This equation has an uncertainty (based on two standard deviations) of 0.74 per cent.

2.3 Calibration in Gas

The Venturi tubes were calibrated in gas in the UKAS-accredited National Standard facility for high-pressure gas flow measurement at two static pressures, 20 bar and 60 (or 70) bar, and the data are presented in Figures 2 – 5. All the gas data were collected in air except the data for 100 mm for b = 0.4 from Jordan Kent Metering Systems/Seiko, which were collected in nitrogen. Since there are two 100 mm Venturi tubes for b = 0.4, 0.6 and 0.75 the ones from Jordan Kent Metering Systems/Seiko are described as '100 mm' and those from Crane Perflow are described as '100 mm*'. In Figure 4 'Yokogawa DP' and 'Mensor DP' refer to the devices used to measure the differential pressure; they were used for two separate calibrations. The data collected in gas are more scattered than those taken in water. There are peaks and troughs in the data sets. In general better agreement is obtained between the two sets of data obtained at different static pressures when the data are fitted against Reynolds number; however, it is clear that the location of the peaks and troughs is a function of the throat velocity. In all data fitting in this paper the points for which $\Delta p/p_1 > 0.08$ were excluded since these points displayed a reduction in discharge coefficient from what would have been expected from other data from the same Venturi tube. It is assumed that this effect is due to expansibility effects which are not incorporated in the expansibility equation. The difference is, however, less than the predicted uncertainty of e_1 in ISO 5167-1.

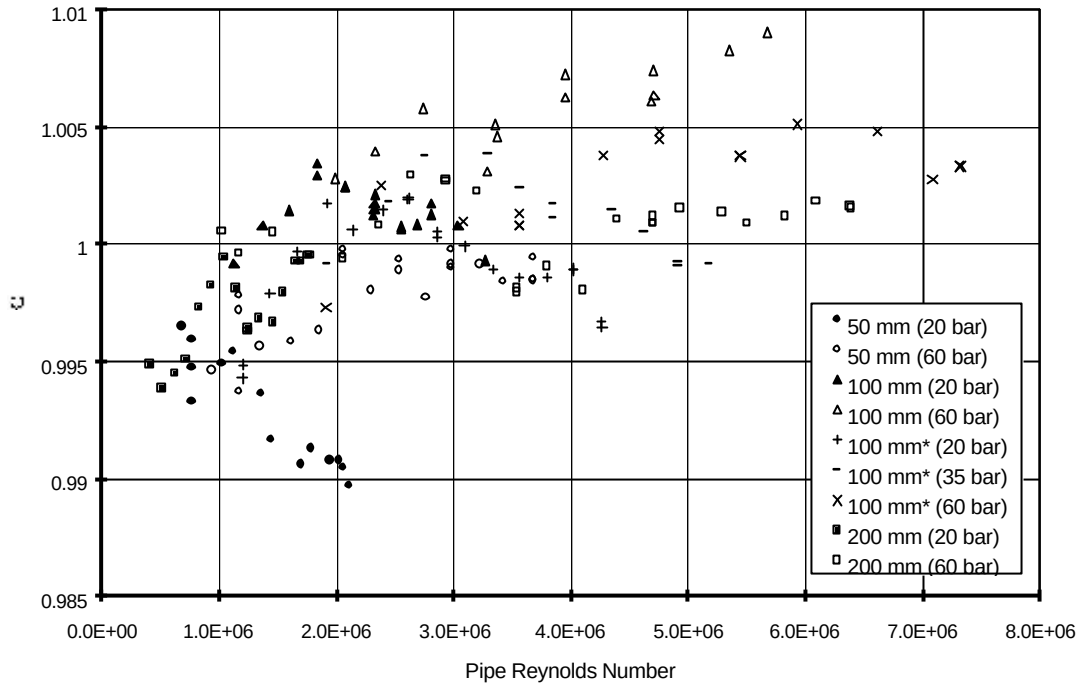

Figure 2 Calibration in gas against Reynolds number: beta = 0.4

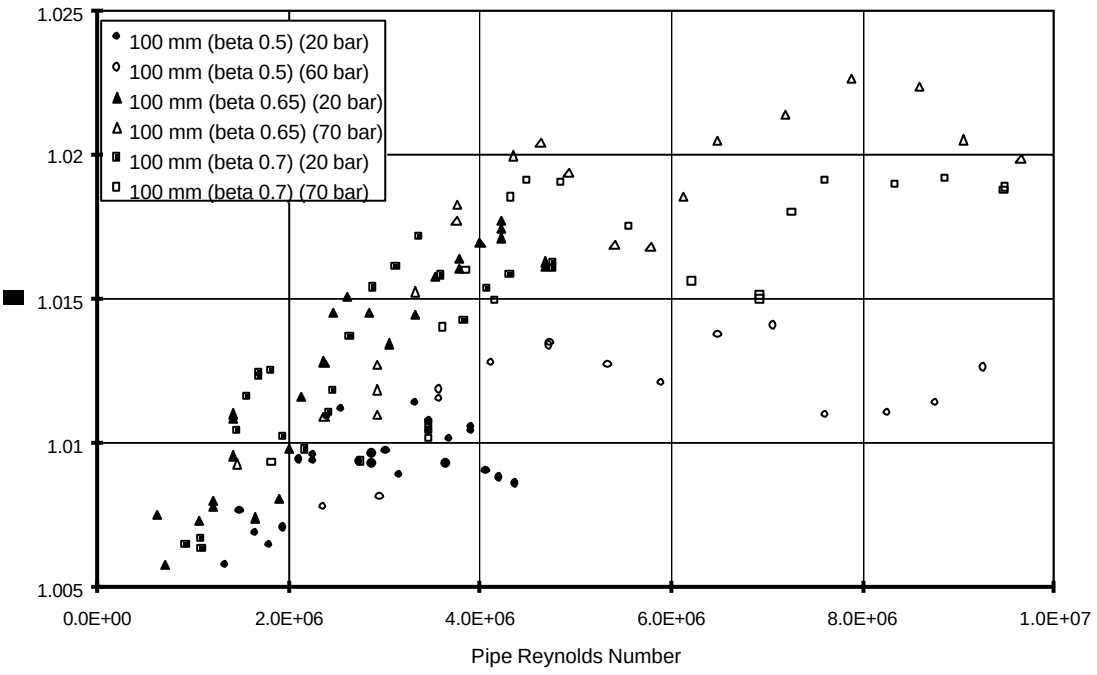

Figure 3 Calibration in gas against Reynolds number: beta = 0.5, 0.65 and 0.7

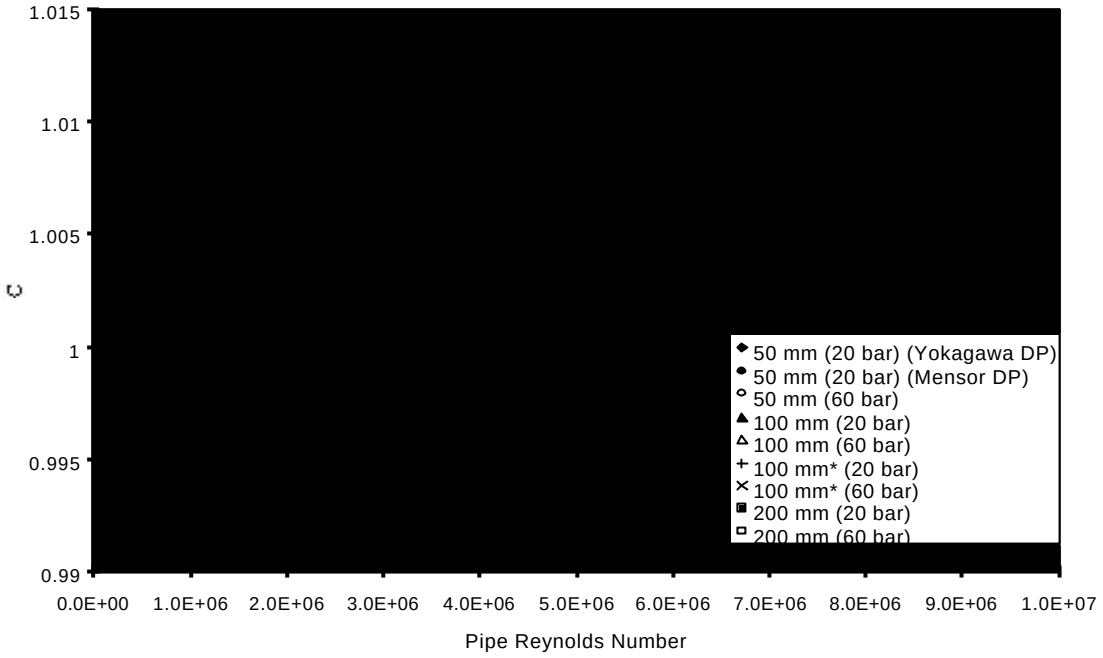

Figure 4 Calibration in gas against Reynolds number: beta = 0.6

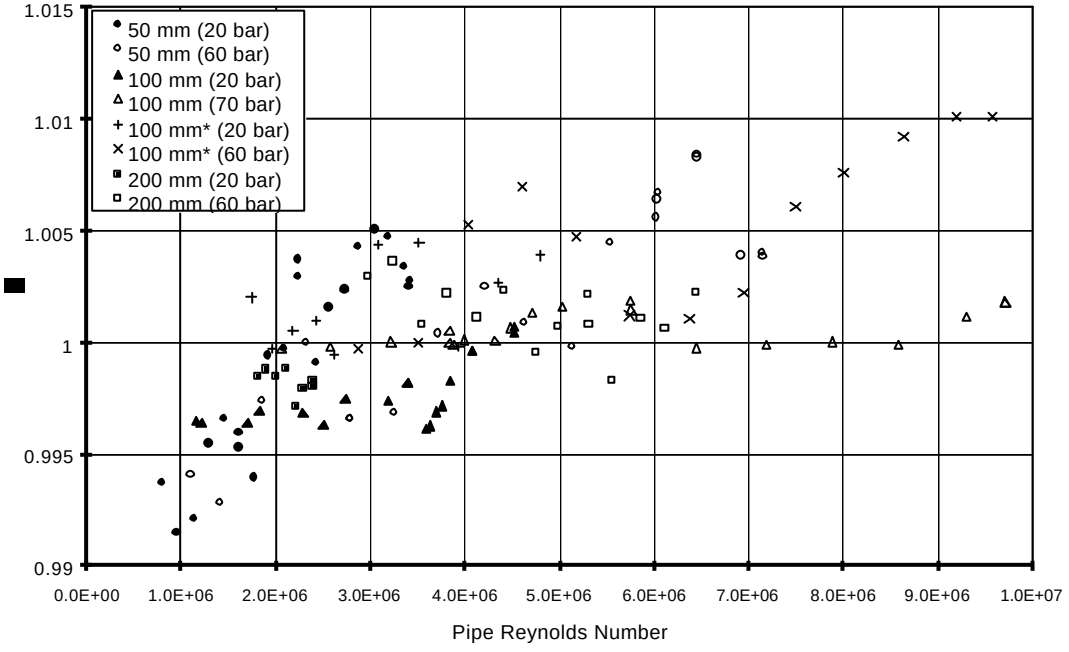

Figure 5 Calibration in gas against Reynolds number: beta = 0.75

2.4 Static Hole Error

In order to fit the gas data it is helpful to observe that some of the variation in C can be removed by examining $C - C_{water}$ where C_{water} is the mean value for the water data for that Venturi tube as shown in Figure 1. A possible cause for the change in discharge coefficient from that obtained in water is static hole error. Static hole error is the effect that pressure tappings of finite size do

not measure the pressure which would have been measured using an infinitely small hole. The effect of static hole error is that the measured pressure using a pressure tapping is higher than the static pressure would have been if the tapping had not been present. This effect is considered in many papers (e.g. Franklin and Wallace [4] and Gibson et al. [5]). If the increase in measured pressure is denoted by e and the wall shear stress by t, then

$$\frac{e}{t} = f(Re_{tap}), \tag{2}$$

where Re_{tap} is the tapping hole Reynolds number defined by

$$Re_{tap} = \frac{u_t d_{tap}}{n}, \tag{3}$$

d_{tap} is the tapping diameter, n is the kinematic viscosity, u_t is the friction velocity, $\sqrt{(t / r)}$, and r is the density. Because the velocity and therefore the wall shear stress are much higher in the throat than in the entrance cylinder the static hole error leads to a reduction in the measured differential pressure and an increase in the measured value of C. To calculate the static hole error it is necessary to have an estimate of the relationship between t and $\overline{u}$, the mean velocity at the tapping plane. Following Schlichting [6] this is expressed in terms of the friction factor, l, where

$$t = \tfrac{1}{8} l r \overline{u}^2. \tag{4}$$

In a standard Venturi tube in both tapping planes Lindley [7] made measurements of t from which l can be deduced. In the entrance cylinder l appears to become asymptotic to 0.012 as Reynolds number increases. For $10^6 < Re_D < 10^7$ and $k/D = 5 \times 10^{-5}$ l will always be within 10 per cent of 0.012 in a straight pipe according to the Moody Diagram (see Schlichting); so it seems an appropriate value to use. In the throat Lindley's measurements of l are approximately 18 per cent higher than would be obtained in a straight pipe of the same relative roughness and Reynolds number; so in determining the static hole error a figure of 0.015 has been used (for $10^6 < Re_d$ and $k/d = 10^{-4}$, $1.18l$ will always be within 6 per cent of 0.015 according to the Moody Diagram).

On this basis (and assuming incompressible flow) the predicted value of the total reduction in differential pressure, e_{total}, is given by

$$e_{total} = \tfrac{1}{8}\overline{u}_{throat}^2 r(0.015 f(Re_{tap,throat}) - 0.012 b^4 f(Re_{tap,up})), \tag{5}$$

This corresponds to an increase in discharge coefficient of approximately

$$\frac{0.015 f(Re_{tap,throat}) - 0.012 b^4 f(Re_{tap,up})}{8(1-b^4)}. \tag{6}$$

In deriving an equation it is necessary to consider the change in C from that found in water. Towards the top of a calibration in water a typical value of $Re_{tap,throat}$ is 3000 at which f is approximately equal to 3.8; so f is written as f^* + 3.8 where $f^*(3000)$ is equal to 0. In water $Re_{tap,up}$ will be less than 3000, but the coefficient of f will be larger than 0.012. Assuming that

$$f^* = a(e^{-nRe_{tap}} - e^{-3000n}) \quad \text{for } Re_{tap} > 3000 \tag{7}$$

the measured values of C - C_{water} can be fitted, and the best fit of f^* to the gas data is

$$f^* = \begin{cases} 7.165 - 8.839e^{-0.00007\,Re_{tap}} \text{ for } Re_{tap} > 3000 \\ 0 \quad \text{for } Re_{tap} \le 3000. \end{cases} \tag{8}$$

This fit has an uncertainty based on two standard deviations of 0.0074. The true static hole error (rather than the difference between the static hole error in high-pressure gas and that in water) is based on

$$f = 10.965 - 8.839e^{-0.00007\,Re_{tap}} \text{ for } Re_{tap} > 3000 \tag{9}$$

and is shown in Figure 6. Moreover, when the uncertainty of the complete equation (from Equations (1) and (6))

$$C = 0.9878 + 0.0123b + \frac{0.015 f^*(Re_{tap,throat}) - 0.012 b^4 f^*(Re_{tap,up})}{8(1-b^4)} \tag{10}$$

with f^* given by Equation (8) is considered, the uncertainty (based on two standard deviations) of the complete database of values of C in gas is 1.24 per cent.

Equation (9) is not inconsistent with the data in Figure 6 (see [5] for the CFD and [8] – [11] for the other data; the CFD results from many analyses have been represented by curve fits, as the sets of results were in good agreement with one another). This is encouraging in that there is a physical explanation for the discharge coefficient values measured in gas. Results at high Reynolds numbers, however, depend on other parameters besides Re_{tap}. This can be seen not only in the work done for this paper but also in the other experimental results, which are very varied at high Reynolds numbers, whereas (see [5]) good agreement between experimental data has been achieved at the Reynolds numbers obtained in water. Moreover, the cause of the peaks and troughs in the data is not clear: they may be the result of unsteady effects (e.g. acoustic effects), whereas the basic static hole error is a steady effect. These unsteady effects may lead not only to peaks and troughs, but also to a change in the static hole error from its basic value.

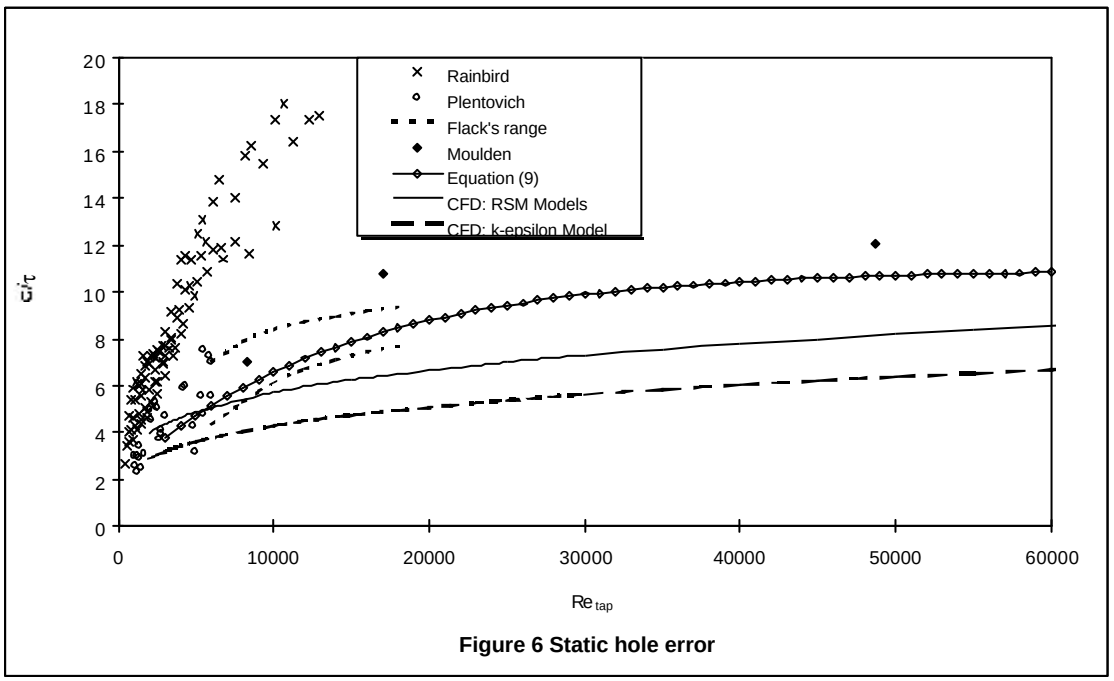

Figure 6 Static hole error

2.5 Practical Equations

An alternative method of presenting the data which is easier to use than the method in Section 2.4 is to observe that the upstream static hole error term is much smaller than the throat term and that therefore it is possible simply to correlate the data with the throat tapping Reynolds number; the simplest presentation of this is to define the Venturi throat tapping Reynolds number

$$Re^* = \frac{d_{tap}}{d} Re_d \,. \tag{11}$$

The data for $C - C_{water}$ can then be plotted against Re^*, as shown in Figure 7.

Fitting the gas data for $C - C_{water}$ gives:

$$C - C_{water} = \begin{cases} 0.0133 - 0.0169e^{-0.4(Re^*/10^5)} & Re^* > 60000 \\ 0 & Re^* \le 60000 \end{cases} \tag{12}$$

This is shown in Figure 7. It has an uncertainty (based on two standard deviations) of 0.0074. When the corresponding overall equation

$$C = \begin{cases} 1.0011 + 0.0123b - 0.0169e^{-0.4(Re^*/10^5)} & Re^* > 60000 \\ 0.9878 + 0.0123b & Re^* \le 60000 \end{cases} \tag{13}$$

is compared with the database for C obtained in gas, it has an uncertainty (based on two standard deviations) of 1.23 per cent.

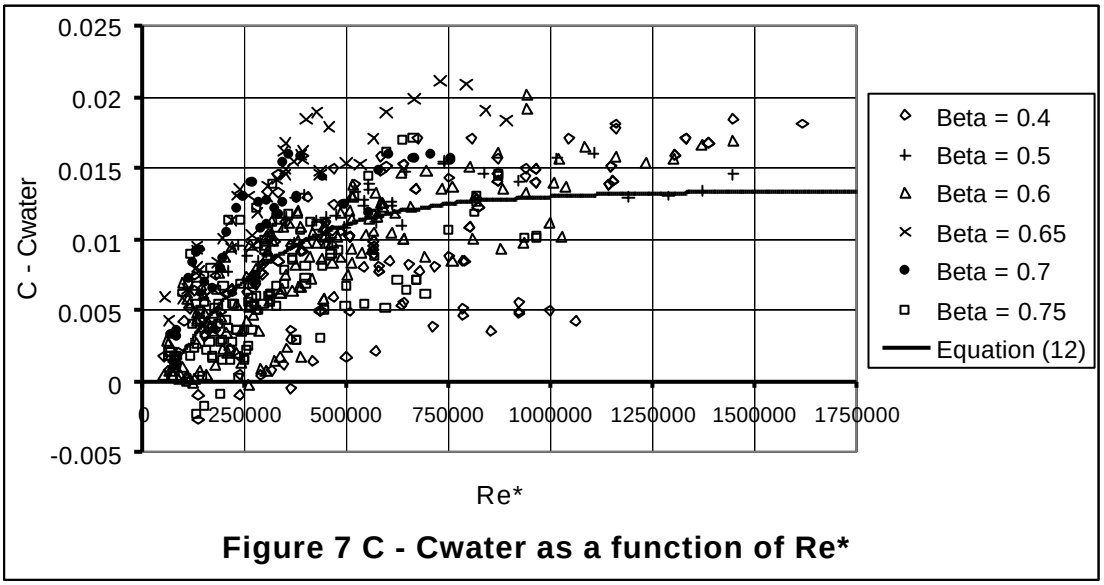

Figure 7 C - Cwater as a function of Re*

3 EFFECTS OF ROUGHNESS

3.1 Introduction

The experimental work described above was carried out on new Venturi tubes. However, there are no guidelines to assist the engineer to predict the through-life performance of Venturi tubes. Operating in a harsh environment (e.g. in flows containing hydrogen sulphide and erosive sand

particles) the internal geometry of the Venturi tube may deteriorate. In particular the Venturi tube may roughen. This will affect the accuracy of the flow measurement. Very many companies were approached to discover how Venturi tube roughness might change with time as a result of surface erosion and corrosion. Only a small amount of information was available, and it was not possible to produce a general theory of how Venturi tube roughness and thus discharge coefficient might change with time. However it was possible to compute the effect of given values of surface roughness on the performance of Venturi tubes. The computer code used was FLUENT 5.

A baseline in which both pipe R_a/D and Venturi tube R_a/d are equal to 10^{-5} was chosen as representative of a very smooth pipe or Venturi tube. This gives values of R_a of 1.5 μm for a 152 mm ID pipe, and 1.1 and 0.6 μm for Venturi tubes of b = 0.75 and 0.4 respectively.

The effect of roughening the Venturi tubes and the upstream pipes was investigated by setting the relative roughness values to 10^{-4}, 10^{-3} and 10^{-2}. The effect of rounding the upstream corner between the throat and the convergent section was also investigated in this work.

3.1.1 Dimensions of the Venturi tubes

The Venturi tubes simulated in this work had diameter ratios of 0.4, 0.6 and 0.75 with an inlet pipe diameter (D) of 152 mm. The convergent and divergent angles were 21° and 15° respectively. The computational mesh extended to the end of the divergent section, except for the b = 0.4 Venturi in which the divergent section was terminated when it had expanded to a diameter of 120 mm. The surface roughness of the Venturi tube walls was set to a constant value throughout, from 152 mm (one diameter) upstream of the convergent section to the end of the divergent section. The upstream pipe was also of a constant (but different) roughness: it joined on to the Venturi tube 152 mm upstream of the upstream end of the convergent section.

3.1.2 Definition of Reynolds Number and pipe diameter

In order to calculate a discharge coefficient it is necessary to know the diameter of the pipe (D) and the diameter of the throat of the Venturi tube (d). Defining these values for a perfectly smooth Venturi tube is straightforward. However, a rough Venturi tube will have an uneven surface and therefore a maximum and minimum diameter, as shown in Figure 8. If the surface is very rough the surface roughness can significantly affect the cross sectional flow area. In the most extreme case considered in this work the cross sectional area of the throat based on the minimum diameter is 12.5% less than that based on the maximum diameter.

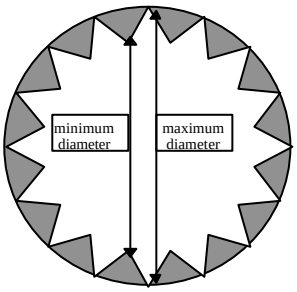

Figure 8 - Cross section through a very rough pipe

Erosion will remove material from the Venturi tube's walls whereas corrosion may act effectively to add material. Either the maximum or the minimum diameter could therefore be used in calculating the discharge coefficient, depending on whether erosion or corrosion is being considered. In this work, the diameters used to calculate discharge coefficients are those of a perfectly smooth Venturi tube. Roughness is assumed to be caused by adding material to the inner surface of the Venturi tube. The change in cross sectional area caused by this additional material is neglected.

Throughout this Section of the paper pipe Reynolds numbers are used. Where dimensional results are provided the pipe diameter, D = 152 mm. To carry out calculations k has been evaluated on the basis that $k = \pi R_a$.

3.2 Mesh Sensitivity Analysis and Validation

3.2.1 Validation of pipe flow simulations

The first step in this work was to confirm that the CFD code could correctly simulate the effects of surface roughness in fully developed pipe flow. This was done by comparing CFD predictions against the widely accepted, experimentally derived rough pipe flow equations given in Schlichting [6]. All CFD simulations of pipes and Venturi tubes simulated turbulence effects using the Reynolds Stress Model (RSM) with standard wall functions.

At a Reynolds number of 2 x 10^7 the maximum difference in pressure drop between the CFD and Schlichting's results was about 3.6%. The velocity and turbulence profiles from these initial predictions were used as inlet boundary conditions for the simulations of the Venturi tubes.

3.2.2 Initial Venturi tube simulations - mesh sensitivity study

Once it had been established that the CFD code could adequately model roughness effects (provided that the wall cell height was larger than the roughness height), it was important to assess the effect of cell size and distribution on the predictions. The first mesh arrangement studied (Mesh Configuration A) had square cells in the throat. The effect that varying the cell size had on discharge coefficient was assessed, as summarised in Tables 1 and 2.

Table 1 - Predicted discharge coefficient for a range of mesh sizes. β = 0.4079, inlet pipe roughness $R_a/D = 10^{-5}$, $Re_D = 2 \times 10^7$

	Mesh Cell Size			
Venturi Tube R_a/d	**4 mm**	**2 mm**	**1 mm**	**0.5 mm**
10^{-2}	0.926	0.926		
10^{-3}	0.973	0.963	0.956	0.956
10^{-4}	0.986	0.981	0.978	0.976
10^{-5}	0.990	0.989	0.987	0.986
0	0.991	0.992	0.992	0.991

Table 2 - Predicted discharge coefficient for a range of mesh sizes. Venturi tube β = 0.75, inlet pipe roughness $R_a/D = 10^{-5}$, $Re_D = 2 \times 10^7$

	Mesh Cell Size			
Venturi tube R_a/d	**4 mm**	**2 mm**	**1 mm**	**0.5 mm**
10^{-2}	0.919	0.932		
10^{-3}	0.960	0.953	0.950	0.960
10^{-4}	0.981	0.979	0.976	0.980
10^{-5}	0.990	0.990	0.988	0.987

It can be seen from Tables 1 and 2 that a 1 mm mesh produces a reasonably grid independent solution. As the roughness increases the spread in the computed values increases. The Configuration A 1 mm mesh was therefore used as the standard mesh in further work.

Unfortunately, the Configuration A mesh was unsuitable when the roughness height exceeded the wall cell height (when Venturi tube $R_a/d = 10^{-2}$). A new mesh configuration with wall cells whose height is increased relative to the dimensions of the other cells (and to their own width)

was tested for these cases (Mesh Configuration B). The size of the wall cells was set to be twice the maximum roughness height, as recommended by the CFD code vendors, and the size of the internal cells was varied, as shown in Tables 3 and 4. Again, it was found that a reasonably grid independent solution could be obtained by setting the size of the internal cells to be 1 mm.

Table 3 - Predicted discharge coefficient for a range of mesh configurations. b = 0.4079, inlet pipe $R_a/D = 10^{-5}$, Venturi tube $R_a/d = 10^{-2}$, $Re_D = 2 \times 10^7$

Height of wall cells (mm)	Size of other cells in mesh (mm)	Discharge Coefficient
4	4	0.926
2	2	0.926
5	2	0.931
5	1	0.933
5	0.5	0.933

Table 4 - Predicted discharge coefficient for a range of mesh configurations. b = 0.75, inlet pipe $R_a/D = 10^{-5}$, Venturi tube $R_a/d = 10^{-2}$, $Re_D = 2 \times 10^7$

Height of wall cells (mm)	Size of other cells in mesh (mm)	Discharge Coefficient
4	4	0.919
2	2	0.932
10	1	0.921
10	0.5	0.922

3.2.3 Validation of Venturi tube simulations

The CFD predictions of flow through a Venturi tube were found to exhibit the correct qualitative behaviour. Spikes occur in the pressure profile along the wall at the corners between the full bore section, the convergent section, the throat and the divergent section just as has been observed in the experimental measurements of Lindley [7] and in earlier CFD [12] (see 3.3.5).

Tables 5 and 6 compare the discharge coefficients of two corroded Venturi tubes described by Spencer and Thibessard [13] against the CFD predictions. In making these comparisons for both comparisons it has been assumed that the mean thickness of the rust deposit on the Venturi tube is equal to the equivalent sand roughness height. In Table 5 both the experimental and CFD values of discharge coefficient are corrected to allow for the additional thickness of the rust deposit, whereas all values in Table 6 are uncorrected. Spencer and Thibessard did not indicate the Reynolds number corresponding to the experimental discharge coefficients given in Table 6. The CFD predictions showed a constant value of discharge coefficient over the range of Reynolds numbers modelled.

Table 5 - Comparison of the experimental results of Spencer and Thibessard and the CFD predictions at a pipe Reynolds number of 10^6.

	D (m)	b	Deposit Thickness (mm)	R_a/d	C of "clean" Venturi tube	C of "corroded" Venturi tube	% Shift in C
Experiment	0.1	0.707	30 (mean)		0.995	0.987	-0.8
CFD	0.152	0.75	36	10^{-4}	0.988	0.979	-0.9
Corrected CFD	0.152	0.75	36	10^{-4}	0.988	0.980	-0.8

Table 6 - Comparison of the experimental results of Spencer and Thibessard and the CFD predictions

	b	Deposit Thickness (mm)	R_a/d	C of "clean" Venturi tube	C of "corroded" Venturi tube	% Shift in C
** Experiment	0.5	100		1.002	0.992	-1.0
CFD	0.4	100	5.24×10^{-4}	0.986	0.968*	-1.8
CFD	0.6	100	3.49×10^{-4}	0.987	0.972*	-1.5
CFD	0.75	100	2.79×10^{-4}	0.988	0.973*	-1.5

* interpolated values ** Venturi diameter D = 152 mm

Tables 5 and 6 show that the CFD predictions match the experimental data of Spencer and Thibessard quite well. However, the comparisons have required assumptions to be made about the nature of the surface roughness and its effective height: the effective roughness height in the experiments is probably smaller than the thickness of the deposit; so it would be expected that the computations, which use the deposit thickness as the roughness height, would give a greater magnitude of shift than the experiments. Moreover, if corrections for static hole error were made agreement with experiment would be considerably improved.

3.3 The Effect of Various Parameters on Discharge Coefficient

The optimised meshes described in Section 3.2 were used to study the effects of varying Venturi tube roughness height, Venturi tube roughness type, pipe roughness height, Reynolds number and the convergent profile on discharge coefficient C.

3.3.1 Effect of Venturi tube roughness height

Table 7 - Predicted discharge coefficient for a range of Reynolds numbers and Venturi tube roughness heights: b = 0.4, inlet pipe $R_a/D = 10^{-5}$

R_a/d / Re_D	0	10^{-5}	10^{-4}	10^{-3}	10^{-2}
10^6	0.987	0.987	0.979	0.956	0.961
5×10^6	0.990	0.988	0.978	0.956	0.961
2×10^7	0.992	0.987	0.978	0.956	0.933

Table 8 - Predicted discharge coefficient for a range of Reynolds numbers and Venturi tube roughness heights: b = 0.75, inlet pipe $R_a/D = 10^{-5}$

R_a/d / Re_D	0	10^{-5}	10^{-4}	10^{-3}	10^{-2}
10^6		0.988	0.979	0.951	0.918
2×10^7		0.988	0.976	0.950	0.921

Except for two points for R_a/d equal to 10^{-2} increasing the roughness of the Venturi tube caused a decrease in the discharge coefficient, as shown in Tables 7 and 8. The pressure spike at the corner between the convergent section and the throat is smaller for rough Venturi tubes, and there is a significant pressure loss in the throat itself. These factors reduce the pressure at the throat tapping, increasing the measured pressure difference across the Venturi tube, thus reducing C.

In β = 0.4 Venturi tubes at higher Reynolds numbers, increasing R_a/d to 10^{-2} causes an apparent increase in C. However, this behaviour should be viewed with some caution as mesh

configuration B (used when R_a/d or R_a/D is equal to 10^{-2}) appears to cause significant errors, as discussed in Section 3.4.

3.3.2 Effect of Reynolds Number

For smooth Venturi tubes, increasing Reynolds number causes an increase in C: this can be seen in Table 7 for b = 0.4; for b = 0.75 C increases from 0.988 when $Re_D = 10^6$ to 0.992 when $Re_D = 2 \times 10^7$ provided that both the Venturi tube and the upstream pipe are smooth (for the Venturi tube R_a/d = 0 and for the upstream pipe R_a/D = 0). The discharge coefficient at a pipe Reynolds number of 2×10^7 is about 0.5% greater than that at 10^6. However, the discharge coefficient of rough Venturi tubes appears to be independent of Reynolds number over the range tested. The decrease in C shown by the very rough Venturi tube is likely to be associated with numerical errors induced by Mesh Configuration B (see Section 3.4).

3.3.3 Effect of Venturi tube roughness type

In the Fluent 5 CFD code roughness is specified in terms of an actual roughness height and a shape factor C_{Ks}. The C_{Ks} value is varied to account for the shape and distribution of the roughness. For example, a riveted surface which has rivets of height 2 mm could be represented by setting the actual roughness height to 2 mm and C_{Ks} to a representative value. A ribbed surface which has 2 mm high ribs would also be represented by setting the actual roughness height to 2 mm, but a different value of C_{Ks} would be used. Setting C_{Ks} to 0.5 reproduces sand roughness. Unfortunately, very little information is available which links values of C_{Ks} to particular roughness patterns. Figure 9 shows that varying C_{Ks} significantly affects the extent to which discharge coefficient varies with roughness height, particularly for very rough Venturi tubes. This implies that the shift in discharge coefficient caused by, say, 100 μm grooves eroded to run parallel to the flow could differ significantly from the shift caused by 100 μm grooves running across the flow.

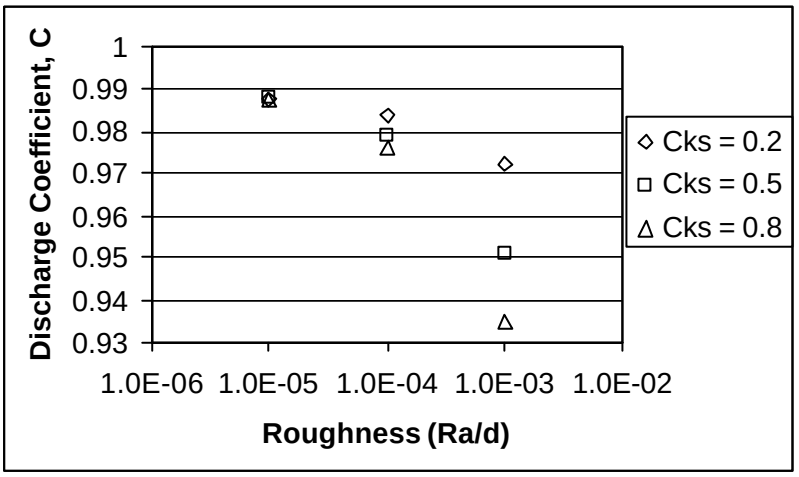

Figure 9 - Variation of discharge coefficient with roughness shape factor, C_{Ks}.b = 0.75, $Re_D = 10^6$.

3.3.4 Effect of pipe roughness

Table 9 - Predicted discharge coefficient for a range of Reynolds numbers and pipe roughness heights: b = 0.4, Venturi tube $R_a/d = 10^{-5}$

R_a/D / Re_D	0	10^{-5}	10^{-4}	10^{-3}	10^{-2}
10^6		0.987	0.987	0.988	0.993
2×10^7	0.985	0.987	0.985	0.985	0.993

Table 10 - Predicted discharge coefficient for a range of Reynolds numbers and pipe roughness heights: b = 0.75, Venturi tube R_a/d =10^{-5}

R_a/D / Re_D	0	10^{-5}	10^{-4}	10^{-3}	10^{-2}
10^6	0.988	0.988	0.990	0.994	0.996
2×10^7	0.987	0.988	0.989	0.990	1.020

Tables 9 and 10 show that increasing the roughness of the pipe upstream of a Venturi tube causes an increase in *C*, and that this effect is small compared with the effect of roughening the Venturi tube itself to an equivalent degree. The effect of pipe roughness increases with b as would be expected.

3.3.5 Effect of altering the convergent profile

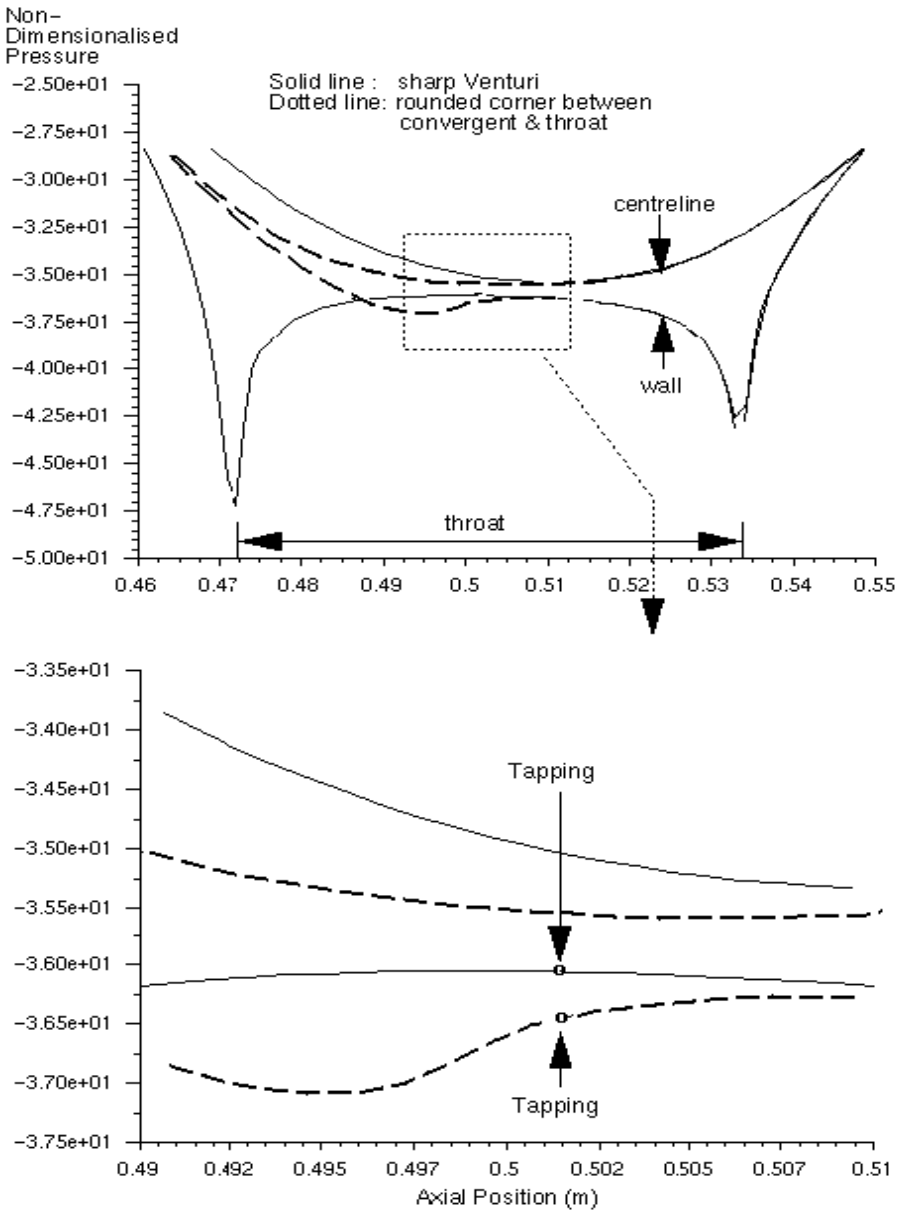

Figure 10 - The pressure profile through the Venturi tube: b = 0.4

Figure 10 shows how rounding the corner between the convergent section and the throat reduces the magnitude of the pressure spike upstream of the throat. (Figure 10 shows the pressure profile for a b = 0.4 Venturi tube with a sharp and with a 4.839d radius corner). However, the rounded corner reduces the straight length of throat upstream of the throat tapping. This causes the spike to recover more slowly, reducing the pressure at the throat tapping, increasing the measured pressure drop and thus decreasing the discharge coefficient.

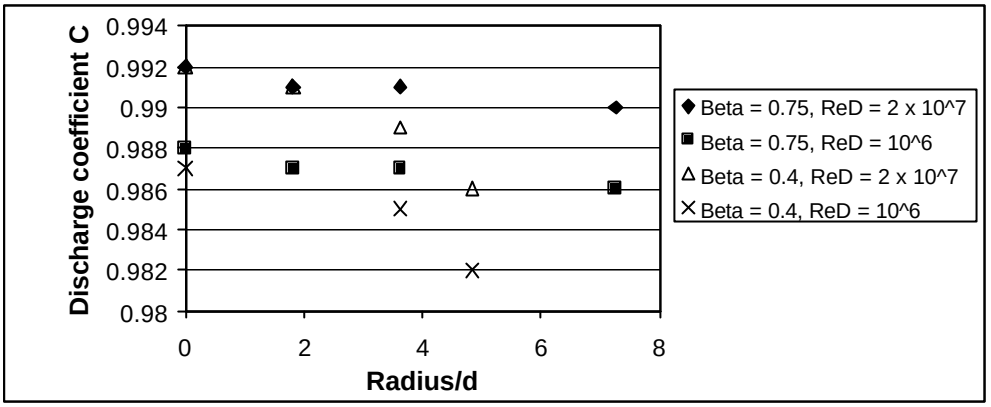

Figure 11 - The effect of rounding the corner between the convergent section and the throat on a smooth Venturi tube downstream of a smooth pipe

Figure 11 shows that rounding the corner of a smooth Venturi tube has a greater effect on small b Venturi tubes. ISO 5167-1 [3] defines an "as cast" Venturi tube as having a fillet radius of 3.625d. For this radius the greatest difference seen between the discharge coefficient of a sharp and rounded Venturi tube was -0.3% (for the b = 0.4 Venturi tube). The difference in discharge coefficient between high and low Reynolds number flows can be seen to remain the same as the radius is increased.

3.4 Difficulties Associated with Modelling Very Rough Venturi Tubes

The results of simulations in which R_a/d is 10^{-3} or less (which use the configuration A mesh) all follow consistent trends. However, simulations involving very rough Venturi tubes or pipes (which use the configuration B mesh) do not follow these trends as closely.

The reason for this inconsistency may be because the CFD code does not calculate mass flow directly, but derives it from axial velocity values. Near the wall, axial velocity changes very rapidly. However, the configuration B mesh has a very large cell near the wall, and this interferes with the numerical integration method used to derive mass flow. Although velocity, pressure and turbulence values may be accurately predicted, the derived mass flow value appears to be consistently over-predicted, causing an over-prediction in values of C of up to 1.35%.

This over-prediction of C, although not large, is enough to confuse some of the trends seen. Values of C predicted for very high roughness pipes or Venturi tubes should therefore be viewed with caution.

Additional complications are caused by the fact that for very rough Venturi tubes, the reduction in cross sectional area of the throat caused by the roughness (assuming roughness is caused by a material being deposited on the Venturi tube's surface) significantly affects the discharge coefficient. As stated in Section 3.1.1 for this work the diameters used in calculating discharge coefficient have been defined as the original (uncorroded/smooth/clean) dimensions of the Venturi tube. If the thickness of the deposited material is accounted for by using the minimum throat diameter instead of the maximum the discharge coefficient is increased, as shown in Table 11.

Table 11 - Shift in discharge coefficient caused by accounting for the reduction in Venturi tube diameter caused by the wall roughness

Venturi tube Roughness (R_a/d)	% change in C
10^{-2}	+ 12.6
10^{-3}	+ 1.26
10^{-4}	+ 0.126
10^{-5}	+ 0.0126

The sensitivity of Venturi tube meters to burrs around the tappings is well known. However, erosion or corrosion severe enough to cause roughness R_a/d values of 10^{-2} will almost certainly distort the effective shape of the tapping, thus altering the static hole error. Indeed, at these roughness levels it is conceivable that tappings could be completely blocked. How the static hole error varies with erosion or corrosion is not known.

Finally, it should be borne in mind that, as described in Section 3.3.3, both the distribution and the type of roughness have a significant effect on the discharge coefficient. As roughness increases, the type of roughness becomes increasingly important.

4 CONCLUSIONS

Fifteen Venturi tubes of standard design of a wide variety of diameters and diameter ratios have been made and calibrated in water and high-pressure gas, and an equation for the discharge coefficient in water has been obtained with an uncertainty of 0.74 per cent. This uncertainty is derived from the mean values of discharge coefficient for each Venturi tube and is based on 2 standard deviations of these mean values about the equation. In gas the situation is considerably more complicated. The recommended equation is Equation (13) with Re^* defined in Equation (11). This has an uncertainty of 1.23 per cent. The physical basis of this equation is static hole error theory. This provides a partial explanation of the measured discharge coefficients. Given the problems with the use of Venturi tubes in gas found in earlier work, this uncertainty is considered to be good. Further work is being undertaken: work on the effect of modifications to the tappings is given in References [14, 15] and on the effect of changing the convergent angle of the Venturi tube in Reference [16].

In addition to the experimental work with new Venturi tubes the effect of roughening the Venturi tubes and the upstream pipes has been investigated using computational fluid dynamics. The results of this study suggest that a very rough Venturi tube could be in error by more than 5%. Upstream pipe roughness has a smaller effect on discharge coefficient, causing it to increase, whereas roughening the Venturi tube causes its discharge coefficient to decrease. The discharge coefficient for rough Venturi tubes is independent of the Reynolds number over the range tested. Hydraulically smooth Venturi tubes show a slight increase in discharge coefficient with increasing Reynolds number.

The discharge coefficient is sensitive to changes in the Venturi tube's dimensions caused by erosion or corrosion, particularly changes in the throat diameter. An even layer of material 152 μm thick will reduce the apparent discharge coefficient of a b = 0.4, 152 mm Venturi tube by 1.0% simply by reducing the cross sectional area of the throat. Equally, erosion of the throat will act to increase C.

The effect of rounding the upstream corner between the throat and the convergent section was also investigated in this work. In an extreme case, in which the rounding almost reaches the throat tapping, the shift in C could exceed -0.5%. However, in reality erosion to this degree is also likely to alter the tapping shape, further complicating the situation.

Based on the information from this study, a corroded Venturi tube will have a reduced discharge coefficient and the flow will be over-measured. An eroded Venturi tube in which the bore is not re-measured will have a reduced discharge coefficient owing to its increased roughness (and the rounding of the upstream corner) but an apparently increased one owing to the change in the throat diameter. The eroded Venturi tube will therefore either over- or under-measure depending on the nature, rate and distribution of the erosion.

ACKNOWLEGDEMENTS

The work described in Section 2 of this paper was carried out as part of the Flow Programme, under the sponsorship of the National Measurement System Policy Unit of the United Kingdom Department of Trade and Industry. Their support is gratefully acknowledged.

The work described in Section 3 was funded by a Joint Industry Project supported by Elf Exploration, Jordan Kent Metering Systems/Seiko, Mobil North Sea, and Shell International. Their support is gratefully acknowledged.

This paper is published by permission of the Director, NEL.

REFERENCES

[1] JAMIESON, A. W., JOHNSON, P. A., SPEARMAN, E. P., and SATTARY, J. A. Unpredicted Behaviour of Venturi Flowmeter in Gas at High Reynolds Numbers. In Proc. 14th North Sea Flow Measurement Workshop, Peebles, Scotland, paper 5, 1996.

[2] Van WEERS, T., Van Der BEEK, M. P., and LANDHEER, I. J. C_d - factor of Classical Venturi's: Gaming Technology? In Proc. 9th Int. Conf. on Flow Measurement, FLOMEKO, Lund, Sweden, pp 203-207, 1998.

[3] INTERNATIONAL ORGANIZATION FOR STANDARDIZATION. Measurement of fluid flow by means of orifice plates, nozzles and Venturi tubes inserted in circular cross-section conduits running full. ISO 5167-1, Geneva: International Organization for Standardization, 1991.

[4] FRANKLIN, R. E., and WALLACE, J. M. Absolute measurements of static-hole error using flush mounted transducers. J. Fluid Mech. **42** (1), pp 33 – 48, 1970.

[5] GIBSON, J. J., READER-HARRIS, M. J., and GILCHRIST, A. CFD analysis of the static hole error caused by tappings in Venturimeters operating in high-pressure gas. In Proc. 3rd ASME/JSME Joint Fluids Engineering Conference, San Francisco, FEDSM99-7149. New York: American Society of Mechanical Engineers, 1999.

[6] SCHLICHTING, H. Boundary Layer Theory. New York: McGraw-Hill, 1960.

[7] LINDLEY, D. Venturimeters and boundary layer effects. PhD Thesis, Cardiff: Dept. of Mech. Eng., Univ. Coll. of South Wales and Monmouthshire, 1966.

[8] FLACK, R. D., Jr. An experimental investigation of static pressure hole errors in transonic flow with pressure gradients. In Proc. Southeast Sem. on Thermal Science, pp 364 – 378, 1978.

[9] MOULDEN, T. H., WU, F. G., COLLINS, H. J., RAMM, H., WU, C. I., and RAY, R. Experimental study of static pressure orifice interference. AEDC TR-77-57, 1977.

[10] PLENTOVICH, E. B., and GLOSS, B. B. Orifice-induced pressure error studies in Langley 7 by 10 foot high-speed tunnel. NASA Tech. Paper 2545, 1986.

[11] RAINBIRD, W. J. Errors in measurement of mean static pressure of a moving fluid due to pressure holes. Quart. Bull. Div. Mech. Eng., Nat. Res. Council, Canada, Rep. DME/NAE. No. 3, 1967.

[12] SATTARY, J. A., and READER-HARRIS, M. J. Computation of flow through Venturi meters. In Proc. 15th North Sea Flow Measurement Workshop, Paper 26, Norway, 1997.

[13] SPENCER, E. A., and THIBESSARD, G. A comparative study of four classical Venturi meters. In Flow Measurement in Closed Conduits, Proc of Symposium held at National Engineering Laboratory, Vol. 1, Paper C3, pp 279-316, September 1960.

[14] READER-HARRIS, M. J., BRUNTON, W. C., GIBSON, J. J., HODGES, D., AND NICHOLSON, I. G. Venturi tube discharge coefficients. In Proc. 4th Int. Symposium on Fluid Flow Measurement, Denver, Colorado, 1999.

[15] READER-HARRIS, M. J., BRUNTON, W. C., GIBSON, J. J., HODGES, D., AND NICHOLSON, I. G. Discharge coefficients of Venturi tubes in gas: increasing our understanding. In Proc. Flow Metering for next millennium, Palghat, India, 2000.

[16] READER-HARRIS, M. J., BRUNTON, W. C., GIBSON, J. J., and HODGES, D. Discharge coefficients of Venturi tubes with non-standard convergent angles. In Proc. FLOMEKO 2000, Salvador, Brazil, 2000.